Free glucosylglycerate is a marker of
nitrogen stress in Mycobacterium smegmatis

SCHOLARONE™
Manuscripts

Free glucosylglycerate is a novel marker of nitrogen stress in *Mycobacterium smegmatis*

Volker Behrends[1]*, Kerstin J. Williams[2]*, Victoria A. Jenkins [2], Brian D. Robertson [2], Jacob G. Bundy[1§]

1: Biomolecular Medicine, Department of Surgery and Cancer, Imperial College, London SW7 2AZ, UK

2: MRC Centre for Molecular Bacteriology and Infection, Department of Medicine, Imperial College, London SW7 2AZ, UK

* These authors contributed equally to the work.

RECEIVED DATE

Running head: Nitrogen stress marker in *Mycobacterium smegmatis*

§ Corresponding author.

Tel: +44 (0)20 7594 3039

Fax: +44 (0) 20 759 43226

Email: j.bundy@imperial.ac.uk

ABSTRACT

Nitrogen is an essential element for bacterial growth and as such bacteria have evolved several pathways to assimilate nitrogen and adapt to situations of nitrogen limitation. However, the adaptation of mycobacteria to nitrogen stress and the regulation of the stress response pathways is unknown. Identification of key metabolites produced by mycobacteria during nitrogen stress could therefore provide important insights into mycobacterial survival strategies. Here we used NMR-based metabolomics to monitor and quantify intracellular and extracellular metabolite levels (metabolic footprinting) in *Mycobacterium smegmatis* grown under nitrogen-limiting and nitrogen-rich conditions. There were several metabolic differences between the two conditions: following nitrogen run-out, there was an increase in intracellular α-ketoglutarate and a decrease in intracellular glutamine and glutamate levels. In addition, a sugar-derived compound accumulated in nitrogen-starved cells that was subsequently assigned as glucosylglycerate (GGA). Free GGA production was responsive to nitrogen stress in *M. smegmatis* but not to oxidative or osmotic stress; lack of a functional GGA synthesis pathway slightly reduced growth and decreased ammonium uptake rates under nitrogen-limiting conditions. Hence, GGA could contribute to the fitness of mycobacteria under nitrogen limitation.

KEYWORDS: NMR, nitrogen stress, carbon metabolism, nutrient limitation, metabolic footprinting, glucosylglycerate, glucosylglyceric acid, Mycobacteria

INTRODUCTION

In order to survive, bacteria must be able to sense and adapt to their environment. Conditions encountered by bacteria include fluctuations in the availability of water, oxygen and nutrients, such as nitrogen. The physiological response to nitrogen limitation involves a complex interplay between signalling molecules, transporter proteins, transcriptional regulators and metabolic enzymes, with metabolites often playing a crucial role in relaying and signalling nitrogen limitation. In the well-studied model organism *Escherichia coli* the intracellular ratio of glutamine and α-ketoglutarate levels signal nitrogen status and is thought to be central to the initiation of the nitrogen response, which involves transcriptional control of the NtrC regulon consisting of about 100 genes.[1] α-Ketoglutarate also acts as an effector molecule by binding to signalling proteins such as PII (which in turn affects NtrC phosphorylation)[2] while also directly modulating glucose uptake via the phosphotransferase system.[3] Therefore, the identification and quantification of metabolites during nitrogen limitation is fundamental to understanding the signal mechanisms and key pathways involved in the nitrogen stress response.

The mycobacteria contain both non-pathogenic and pathogenic species including *Mycobacterium tuberculosis*, the etiological agent of tuberculosis (TB) responsible for 2 million deaths per year worldwide.[4] Crucial to its success as a global pathogen is its ability to adapt to various host environments during its life cycle, such as nutrient limitation. However, little is known about the mechanisms or metabolites involved in the nitrogen stress response in mycobacteria.[5] As findings in one bacterial group are not readily transferrable to other species, it is important to study the systems involved in regulating the nitrogen stress response in mycobacteria to elucidate key stress survival pathways and potentially identify novel drug targets. To this end, we studied the nitrogen starvation response in the model mycobacterium *Mycobacterium smegmatis*, a non-pathogenic saprophyte.

Metabolic profiling (metabolomics) has been used to investigate bacterial metabolism for a variety of applications including functional genomics, biotechnology and systems biology. [6, 7] A number of metabolic profiling approaches for both endo- and exometabolome quantification have been employed

to elucidate the metabolic consequences of physiological stresses in prokaryotic organisms. [8-10] Therefore, to further our understanding of the nitrogen stress response of *M. smegmatis*, we employed an untargeted NMR-based metabolic profiling approach to quantify the metabolic changes occurring as the cells adapt to nitrogen limiting conditions. In this report we present novel metabolite changes, including the unexpected finding that free glucosylglycerate (GGA) accumulates in response to nitrogen limitation.

4

MATERIALS AND METHODS

Bacterial strains and growth conditions

We used the strain *Mycobacterium smegmatis* mc²155 (ATCC700084)[11] for initial experiments on nitrogen limitation. The *M. smegmatis gpgS* null mutant (msmeg_*5084::km*) was a gift from Mary Jackson (Colorado State University, Fort Collins, USA). Both strains were grown at 37 °C with shaking at 180 rpm in modified Sauton's minimal medium [12] (without asparagine; ferric citrate replacing ferric ammonium citrate; glycerol reduced to 0.2%) supplemented with 0.0001% $ZnSO_4$ and 0.015% Tyloxapol. Ultra-pure $(NH_4)_2SO_4$ (Sigma) was added as nitrogen source at either 1 mM (nitrogen-limiting) or 30 mM (nitrogen-rich) final concentration. Cells were initially grown to late-log phase in nitrogen rich medium, then washed twice with nitrogen-free medium and used to inoculate nitrogen-limiting or nitrogen-rich medium at an initial OD_{600} of 0.1. Cell growth was monitored by OD_{600} over 24 hrs and cells were sampled for external ammonium concentration at periodic intervals during growth as described below. For metabolomic analysis, cells were sampled as described below at 10 hrs, 11.5 hrs and 13.5 hrs, representing nitrogen depletion and run out in the nitrogen limiting conditions. For nitrogen 'up-shift' experiments, nitrogen limited cultures were spiked with 10 mM $(NH_4)_2SO_4$ at 13.5 hrs and samples taken at 2, 10, 30, 90, and 180 minutes post-spike. To test the influence of carbon source on glucosylglycerate formation, glycerol was replaced with 0.2% (w/v) glucose or 10 mM succinate as indicated. For osmotic stress studies, the medium was supplemented with 0.3 M NaCl. For oxidative stress experiments, the cells were exposed to 5 mM H_2O_2 for 2 hours at 14 hours of growth as previously described.[13] For these alternative carbon source and stress test experiments, all cells were sampled after 16 hrs of growth representing nitrogen run out in the nitrogen limiting conditions.

Determination of nitrogen concentration

Ammonium levels in the growth medium were measured using an Aquaquant ammonium detection

kit (Merck) according to manufacturer's instructions. At each time point cells were pelleted by centrifugation at 16,000 g and the cell supernatants transferred to a new tube. Ammonium concentrations in the cell supernatants were quantified by comparison to a $(NH_4)_2SO_4$ standard curve.

Metabolite sampling and extraction

Samples for exo-metabolome analysis were obtained by centrifuging 500 µl of culture (16,000 g, 1 minute, room temperature). Samples for extraction and endo-metabolome analysis were taken by (1) rapid filtration, (2) total quenching (for labile metabolites), or (3) centrifugation, i.e. unquenched (for metabolite assignment only). All biological experiments to quantify responses were carried out in triplicate as standard.

For rapid filtration, cells were sampled using a protocol adopted from Bolten *et al*.[14] In short, 5 mL of cell suspension were harvested by vacuum filtration (filter: PTFE, 0.45 µm pore size, 47 mm, Pall, stand: Filtersys™, Phenomenex, Macclesfield, UK) and washed once with 5 mL of 0.9% w/v saline. The filter was then transferred as quickly as possible to a pre-cooled (-40 °C) 50 ml reaction tube containing 10 ml methanol:acetonitrile:H_2O (2:2:1, v/v/v) and frozen in liquid nitrogen. For total quenching (i.e. cells not separated from broth), 5 ml of culture were sampled into 20 ml methanol:acetonitrile (1:1, v/v) held at -50 °C and immediately frozen. Unquenched sampling was used to produce a concentrated sample for identification of glucosylglycerate only, i.e. not for any biological response experiments. Here, 30 ml of culture were centrifuged at 3600 g for 10 min. The supernatant was discarded and 5 ml methanol:acetonitrile:H_2O (2:2:1, v/v/v) were added to the pellet, mixed and frozen immediately. All extracts were subjected to two freeze-thaw cycles, dried in a vacuum concentrator (Eppendorf, 45 °C) and resuspended in 1 ml methanol:acetonitrile:H_2O (2:2:1, v/v/v). 90% of the sample was routinely used for NMR, and 10% was used for GC/MS.

Sample preparation

We analysed the exometabolome samples by NMR only, and the endometabolome samples by both NMR and GC-MS. The exometabolome samples were prepared by mixing 480 µl cell-free culture supernatant with 120 µl NMR buffer (5 mM 2,2-dimethyl-2-silapentane-d$_6$-5-sulfonic acid (DSS), 25 mM NaN$_3$ in 100% D$_2$O). For NMR measurements of the endometabolome, the samples were dried in a vacuum concentrator, resuspended in NMR buffer (90% D$_2$O, 1 mM DSS, 5 mM NaN$_3$) and transferred to a 5 mm NMR tube. For GC/MS, samples were derivatised by a two-step methoximation/silylation derivatization procedure.[15] We added 20 ml 1 mM of both 2,3,3-d$_3$-leucine and U-^{13}C-glucose to the samples as derivatisation standards and 3 mg/ml myristic acid-d$_{27}$ for retention time locking. The dried samples were first methoximated using 20 µl of 20 mg/ml methoxyamine hydrochloride in anhydrous pyridine at 37 °C for 90 min followed by silylation with 80 µl N-methy-N-(trimethylsilyl) trifluoroacetamide (MSTFA) at 37 °C for 30 min.

NMR spectroscopy

Spectra were acquired on a Bruker Avance DRX600 NMR spectrometer (Bruker BioSpin, Rheinstetten, Germany), with a magnetic field strength of 14.1 T and resulting ^{1}H resonance frequency of 600 MHz, equipped with a 5-mm inverse probe. One-dimensional spectra were routinely acquired following the approach given in Beckonert *et al.* [16] Briefly, a one-dimensional NOESY pulse sequence was used for water suppression; data were acquired into 64 k data points over a spectral width of 12 kHz, with eight dummy scans and 768 scans per sample. The spectra were apodized (0.5 Hz) and Fourier transform applied, followed by phase correction, in iNMR 3.6 (Mestrelab), and the data then exported as full-resolution spectra to Matlab 2010b (Mathworks) for further analysis. We assigned metabolites by comparison of the chemical shift and multiplicity of resonances with online databases[17,][18], and confirmed assignments by acquiring 2D spectra as appropriate; the assignment of one metabolite, glucosylglycerate, is described in detail. We quantified individual metabolites by integrating the area of characteristic resonances in Matlab.

Spectra acquired for the assignment of glucosylglycerate were acquired on a Bruker Avance DRX600 NMR equipped with a 5 mm cryogenic probe. One-dimensional spectra were acquired as above with 64 scans and eight dummy scans. Two-dimensional correlation (COSY) spectra were acquired with the *cosygpprqf* pulse sequence into 4096 data points x 512 increments with 8 scans per increment over a spectral width of 10.24 Hz. Heteronuclear Single Quantum Coherence (HSQC) spectra were acquired using the *hsqcetgpsi2pr* pulse sequence into 4096 data points x 600 increments with 8 scan per increment over a spectral width of 12 Hz (^{1}H) and 170 Hz (^{13}C), respectively. Heteronuclear multiple-bond correlation (HMBC) spectra were acquired using the *hmbcgplpndprqf* pulse sequence into 4096 data x 256 increments with 160 scans per increment over over a sweepwidth of 10.3 Hz (^{1}H) and 220 Hz (^{13}C), respectively.

GC/MS measurements

GC/MS analysis was performed on an Agilent 7890 gas chromatograph connected to an Agilent 5975 MSD (Agilent Technologies UK Ltd.). Samples were injected with an Agilent 7683 autosampler injector into deactivated splitless liners according to the method of Kind *et al*.[15] Metabolites were assigned using the Fiehn Library[15] with the deconvolution program AMDIS[19] and the quality manually checked and the peaks re-integrated using the add-on Matlab code GAVIN.[20] Metabolite levels were normalised to derivatisation standards and optical density of the cultures.

RESULTS

Changes to the endo-metabolome of Mycobacterium smegmatis *in response to low nitrogen*

We monitored the growth of *M. smegmatis* mc^{2}155 in nitrogen-limiting (1 mM (NH$_4$)$_2$SO$_4$) or nitrogen-rich (30mM (NH$_4$)$_2$SO$_4$) conditions by optical density, and also measured ammonium concentrations in the growth medium. As previously described [21], although initial bacterial growth rates in both conditions were similar, growth continued even after complete depletion of external ammonium in the nitrogen-limiting medium at 12 hrs, albeit at a slower rate than in the nitrogen rich conditions. A similar growth phenotype was observed with glutamine as the sole nitrogen source (data not shown) suggesting this reduced growth rate was a general response to nitrogen limitation.

In order to investigate the metabolic response to nitrogen limitation in *M. smegmatis*, we used NMR to compare the levels of intracellular and extracellular metabolites from bacteria grown in low and high nitrogen-containing medium. Analysis of the exo-metabolome using time-resolved metabolic footprinting (TReF[22]) showed only one clear difference: glycerone increased transiently in the culture supernatant following nitrogen depletion (supplemental Figure S1 in supporting information). In contrast, there were several metabolic differences between the endo-metabolome of cells sampled under the two different nitrogen regimes (Figure 1).

The sampling method had a large effect on which metabolites were detected as nitrogen limitation markers. Cells sampled by centrifugation (no quenching of metabolism) exhibited differences in amino acids like glutamate, glutamine, aspartate and threonine and nucleotide resonances, all of which had increased concentrations under nitrogen rich conditions. Three spectral resonances (designated NR$_1$ to NR$_3$ in Figure 1B, with chemical shifts δ 5.01, δ 4.20, and δ 3.54 ppm) were inversely correlated to nitrogen availability and therefore identified as potential markers of nitrogen limitation (Figure 1A and 1B). We also observed increased, but highly variable levels of glycogen (data not shown; glycogen annotated on NMR spectrum shown in supporting information, supplemental Figure S2). When cells

were sampled by total quenching (simultaneous cooling and extraction of cells and broth), the metabolomic pattern was slightly different. We again observed increases in the concentrations of the amino acids alanine and glutamate under nitrogen-rich conditions, and we also observed increases in trans-aconitate as well as an as-yet unassigned metabolite, with an AB spin system at 2.92 ppm. Several metabolites related to sugar metabolism (glycogen, glucose, glucose-1-phosphate and glyceraldehyde) were elevated under nitrogen-limiting compared to nitrogen-rich conditions. In addition, as for the samples obtained by centrifugation, we observed increases in the resonances NR_1 and NR_2 (NR3 was obscured by resonances from glycerol in the total quenching samples). In terms of absolute signal levels, the biggest intracellular change observed for both sampling regimes in response to nitrogen limitation, was a decrease in glutamate levels and accumulation of the unknown compound (i.e. the resonances NR_1, NR_2, and NR_3).

Identification of glucosylglycerate as a specific nitrogen stress marker

As the stability of NR_1 and NR_2 resonances were confirmed as markers of nitrogen stress using both rapid filtration and total quenching as sampling protocols, we wanted to assign the metabolite involved. We examined extracts of nitrogen-limited cells using GC-ESI-MS (revealing a peak at 21.41 min with the major fragments at m/z 204, 217, and 361) and 2D NMR experiments (TOCSY, HSQC and HMBC, chemical shifts listed in Table 1). Based on the TOCSY we established that the two resonances at δ 5.01 and δ 4.20 ppm originated from two distinct spin systems. The similarity of spin system 1 (δ 5.01 ppm) to the resonances from the disaccharide trehalose (Table 1 and Figure 2), indicated that spin system 1 was glucose. An HMBC experiment revealed that the peak at δ 4.20 ppm had long-range couplings to carbon resonances at δ 100.3 ppm (identical to the chemical shift of the carbon atom bound to the proton with a resonance at δ 5.01 ppm as determined by the HSQC experiment), δ 180.3 ppm and δ 66.3 ppm. As the latter two resonances were indicative of a carboxyl group and a primary hydroxy group, respectively, we tentatively assigned the compound as glucosylglycerate (GGA). Comparison with

literature data for GGA (proton and carbon NMR chemical shifts[23, 24] and GC-EI-MS data[25]) confirmed this assignment.

In order to determine if the GGA response was specific to nitrogen stress or produced as a general stress marker, we performed a series of experiments exposing *M. smegmatis* to other stress conditions. The results confirmed that GGA is a specific marker of nitrogen stress in *M. smegmatis*, at least for the stress conditions studied here (Table 2). In addition, GGA production was not dependent on the use of glycerol as the main carbon source for growth, as the same response was seen when the cells were grown with glucose or succinate as the sole carbon source (Table 2). We also confirmed that the metabolite changes observed in this study and GGA production were directly linked to nitrogen availability, by observing metabolite changes when ammonium was added back into the nitrogen limiting medium after the nitrogen had been exhausted (Figure 3). As expected, nitrogen limitation led to a massive accumulation of GGA inside the cells, associated with a small increase in trehalose. In addition, intracellular α-ketoglutarate increased while most other metabolites decreased. After spiking with nitrogen, the starvation response was reversed, with a sharp decrease in α-ketoglutarate levels, reduction in GGA levels and an increase in glutamate levels. Interestingly, the concentrations of citric acid cycle metabolites downstream of α-ketoglutarate remained depressed after the nitrogen spike, possibly because of the rapid carbon flux of α-ketoglutarate to glutamate, observed following the ammonium spike (Figure 3).

Putative role of GGA in nitrogen stress response

Further evidence that GGA is an important metabolite in the adaptation to nitrogen stress was provided from a global transcriptomic analysis of *M. smegmatis* grown under nitrogen limitation (K. Williams *et al*., unpublished data). The expression levels of the *M. smegmatis gpgS* gene (msmeg_5084), encoding the enzyme catalyzing the first dedicated step in GGA synthesis, were increased approximately 20-fold upon external nitrogen depletion but unchanged in nitrogen excess

(Supplemental Figure S3 in Supporting Information). To characterize the importance of GGA metabolism in nitrogen stress, we obtained an *M. smegmatis* mutant in which the *gpgS* gene was inactivated[26]. This *gpgS* null mutant took up ammonium from the growth medium at a slower rate than the wild-type strain, and had a slight reduction in growth rate compared to the wild-type in nitrogen limiting conditions (Supplemental Figure S4 in Supporting Information). The reduction in growth rate was statistically significant (P = 0.0017, ANCOVA; Supplemental Figure S5 in Supporting Information). We also compared the NMR metabolic profiles of the mutant to the wild-type under high and low nitrogen conditions, approximately six hours after ammonium runout. This confirmed that, as expected, there was no detectable GGA in the mutant samples. The other major metabolites that responded to nitrogen stress were the same as for the wild-type: glutamate decreased, and α-ketoglutarate and trehalose increased; there was also a substantial increase in glycogen (Figure 4A). When the metabolite changes were compared for the mutant with respect to the wild-type in the high-nitrogen and low-nitrogen conditions separately, there were no differences under nitrogen sufficiency, but all four metabolites had altered responses under nitrogen starvation (one-way t test, null mean of fold-change = 1; Figure 4B).

Glutamate is widely used as an osmolyte by many bacterial species[27], but glutamate concentrations tend to decrease under nitrogen limitation[28], as was the case in our current study (Figure 3). Cyanobacteria are known to use GGA as an alternative osmolyte under nitrogen stress.[28] Hence, we investigated whether GGA might play a similar osmotic stress protection role in *M. smegmatis*. However this was not the case: trehalose and not GGA was clearly responsive to osmotic stress (Figure 5).

DISCUSSION

Identification of key metabolite changes and GGA production during nitrogen stress

Our findings show a fundamental switch in the metabolism of *M. smegmatis* in response to nitrogen limitation, with an increase in the intracellular levels of carbohydrates and related compounds (e.g. glycogen, glucose-1-phosphate). We identified the compound with the biggest increase in concentration as glucosylglycerate (GGA) which represents a novel function for this compound in *M. smegmatis*. GGA is thought to mainly function as a terminal group in the sugar chain on the methylglucose lipopolysaccharide (MGLP) in mycobacteria, but its precise role is not known; there are conflicting reports as to its role in the regulation of fatty acid biosynthesis and mycolic acid metabolism. The production of GGA in response to nitrogen availabilityhas not previously been reported in mycobacteria. We confirmed that free GGA was increased by nitrogen stress but not by several other physiological stresses, including osmotic and oxidative stress. A previous study on nitrogen starvation in *M. smegmatis* also highlighted increased levels of glycogen as a metabolic feature of nitrogen limitation, with no change in trehalose concentrations.[29] They did not report an increase in GGA, which could be explained by the fact that they quantified metabolites based on metabolism of radiolabelled ADP-glucose, while GGA is usually synthesised from UDP-glucose.[30]

The putative role of GGA in nitrogen limitation

Our data suggest that glutamate and GGA could act as carbon and nitrogen capacitors that help maintain intracellular homeostasis and survival under nitrogen limitation. The growth kinetics suggest that intracellular concentrations of nitrogen-containing small molecules are largely but not exclusively governed by exogenous nitrogen availability in *M. smegmatis*, as the cells continue to grow even after extracellular nitrogen has been wholly depleted.[21] This suggests that in times of high nitrogen

availability, nitrogen is imported at a rate greater than necessary for growth and stored intracellularly; this store is depleted (and contributes to growth) when extracellular nitrogen has run out. The nature of the putative intracellular nitrogen storage molecule (or molecules) remains to be determined. It is plausible that glutamate, the most abundant nitrogen-containing small molecule, has a role in nitrogen storage and retrieval. Glutamate is initially present at high intracellular concentrations (approximately 700 mM) during growth in nitrogen-rich conditions (based on cell sizes as given by Cox and Cook [31] and Smeulders *et al.* [32]) but levels decrease during nitrogen starvation to about 50 mM. Polyglutamyl storage molecules are common in slow growing mycobacteria, accounting for about 15% of the delipidated cell wall weight in *M. bovis BCG*, but are not found in *M. smegmatis.*[33] In other bacteria such as *E. coli*, intracellular α-ketoglutarate concentrations rise upon nitrogen starvation[1, 3] and growth of *E. coli* in nitrogen-limiting conditions is associated with excretion of significant amounts of α-ketoglutarate into the external medium.[34] This precise response is not exhibited by mycobacteria as metabolite profiling analysis of the culture supernatants did not show any excretion of α-ketoglutarate. In fact, the only NMR-detectable metabolic difference between the nitrogen-limited and nitrogen-rich culture supernatants was a transient increase in glycerone. It is therefore possible that *M. smegmatis* sequesters the resulting carbon intracellularly by increasing the levels of GGA and glycogen. This hypothesis is plausible as the accumulation of GGA is reversible and its levels decrease when nitrogen is replenished. The kinetics of the response to nitrogen replenishment also strongly suggests that α-ketoglutarate functions as a signalling molecule in *M. smegmatis*, as its levels rapidly decrease after nitrogen is added to the medium.

GGA is not essential for growth in nitrogen limiting medium, but confers an advantage

A mutant unable to synthesise GGA showed a slight reduction in growth rate and ammonium uptake in nitrogen limiting conditions compared to wild type. While this shows that GGA is not essential for survival under low nitrogen, it does nonetheless demonstrate a phenotypic effect of the GGA synthesis

pathway under nitrogen stress. It is possible that it could affect its fitness in a relevant ecological situation, e.g. competing for scarce resources in an oligotrophic soil environment.[35] However, it should be borne in mind that competitive fitness is contingent, i.e. it depends on the environment and so is not a fixed quantity for any one strain[36]. More experiments under a range of conditions would be needed to draw a definitive conclusion implicating this pathway as contributing to fitness under nitrogen stress in the natural environment. In addition, GGA also has a role as a head group of a methyl-glucose lipopolysaccharide (MLGP). This polysaccharide is thought to be involved in regulating fatty acid synthesis[30], though recent studies have questioned this role in the physiology of mycobacteria.[26] Whether the relatively high intracellular concentration of MGLP[37] is affected during nitrogen limitation, and what affects this may have on fatty acid synthesis, is beyond the scope of this study. It is also interesting that the mutant has qualitatively the same responses as the wild-type for the major metabolites that change as a result of nitrogen runout: glutamate decreases, and α-ketoglutarate and trehalose both increase. (The increase in glycogen was also more clear-cut than for the wild-type, where the data were variable.) However, quantitatively, the response for N-containing glutamate was damped (a smaller decrease for the mutant on N starvation), whereas the responses for N-free α-ketoglutarate, trehalose, and glycogen were all stimulated (larger increases for the mutant on N starvation). This would tend to support our argument that GGA is acting as a carbon capacitor: the mutant strain upregulates its production of trehalose in particular (a larger absolute concentration change than for α-ketoglutarate and glycogen) to compensate for the lack of GGA. On the other hand, the reduced decrease in glutamate pool size does not so readily fit this hypothesis; however, it still represents further evidence that nitrogen metabolism is perturbed in the Δ*gpgS* mutant, arguing for the importance of the GGA pathway in the response of *M. smegmatis* to nitrogen stress.

In summary, we have determined key metabolite changes in *M. smegmatis* during nitrogen limitation, and identified GGA as a novel marker for nitrogen stress in a mycobacterial species. However the role of GGA in the response of mycobacteria to nitrogen stress still needs to be elucidated. In *M.*

tuberculosis the *gpgS* gene (Rv1208) is annotated as essential for *in vitro* growth [38, 39], so this enzyme might be an important novel drug target. Experiments to monitor GGA production in nitrogen stress and the essentiality of *gpgS* in *M. tuberculosis* are underway.

Supporting Information Available. Supplementary figures showing additional metabolite annotations and timecourses, gene induction, growth curves, and ammonium utilization.

FIGURE LEGENDS

Figure 1. Nitrogen availability alters *Mycobacterium smegmatis* metabolism. Representative ^{1}H NMR spectrum of extracts from (A) nitrogen-limiting and (B) nitrogen-rich cultures. (C) Endometabolome metabolites with the highest fold-change values between cells sampled by total quenching at 10 h and 17 h from nitrogen-limiting and nitrogen-rich cultures, respectively.

Figure 2. Selected region of ^{1}H-^{13}C HSQC spectrum of extracts of *M. smegmatis* mc^{2}155 grown in 1 mM $(NH_4)_2SO_4$ for 17 h. Cells were harvested by centrifugation and washed with 0.85% saline solution prior to extraction. Carbon atoms and proton resonances for GGA and trehalose are marked on the spectrum.

Figure 3. Changes of compound levels in response to nitrogen levels. Cells were harvested by rapid filtration and measured by NMR (glutamine and glutamate for the data represented by color bars; and glucosylglycerate, α-ketoglutarate and glutamate for the data represented by line plots in insets) and

GC/MS (all other compounds). Signal levels for NMR and GC/MS were normalised to the internal standards DSS and $^{13}C_6$-glucose, respectively, as well as cell number (OD_{600}). Colorbars represent $\log_e$ fold-change with respect to signal intensity at first time point.

Figure 4. Responses of metabolites to nitrogen stress in a Δ*gpgS* mutant unable to synthesize glucosylglycerate. A: fold-change values calculated for the low nitrogen samples relative to the high nitrogen samples. B: fold-change values calculated for the Δ*gpgS* mutant relative to the wild-type strain. Filled bars: low nitrogen medium; empty bars: high nitrogen medium. For both A and B, the bars indicate $\log_2$(fold-change) for individual metabolites. Glu: glutamate. AKG: α-ketoglutarate. Tre: trehalose. Glyc: glycogen. ND: not detected by NMR in nitrogen-sufficient conditions. NA: not appropriate to calculate fold-change. Error bars indicate SD (n = 3).

Figure 5. Levels of GGA, glutamate and trehalose under nitrogen-limiting conditions, high nitrogen and low nitrogen with elevated levels of NaCl. (A) Relative levels and (B) intensities. Cells were grown in the indicated conditions for 16 h, harvested by centrifugation and measured by ^{1}H NMR. Error bars = SEM (n=3).

Table 1. Chemical shifts of glucosylglycerate and trehalose.

	proton	$\delta\,^1H$ [ppm]	carbon	$\delta\,^{13}C$
GGA	H_I	5.01	100.29	C1
	H_{II}	3.54	74.41	C2
	H_{III}	3.82	76	C3
	H_{IV}	3.42	72.28	C4
	H_V	3.79	74.99	C5
	H_{VIa}	3.85	63.31	C6
	H_{VIb}	3.75	63.31	C6
	H_{VII}	4.2	81.9	C7
	H_{VIIIa}	3.85	65.94	C8
	H_{VIIIb}	3.85	65.94	C8
	H_{IX}	n.a.	180.29	C9
Trehalose	H_I	5.18	95.98	C1
	H_{II}	3.64	73.83	C2
	H_{III}	3.86	75.32	C3
	H_{IV}	3.44	72.47	C4
	H_V	3.81	74.99	C5
	H_{VIa}	3.86	63.31	C6
	H_{VIb}	3.76	63.31	C6

Table 2. Production of glucosylglycerate by *Mycobacterium smegmatis* under different stress conditions.

Growth phase	Carbon source	Osmotic stress	Oxidative stress	Nitrogen source[1]	GGA detected
log	glycerol	none	none	1 mM AS	no
log	glycerol	none	none	30 mM AS	no
stat	glycerol	none	none	1 mM Gln	yes
stat	glycerol	none	none	30 mM AS	no
stat	glycerol	none	none	1 mM AS	yes
stat	glycerol	none	none	30 mM AS	no
stat	glycerol	0.3 mM NaCl	none	1 mM AS	yes
log	glycerol	0.3 mM NaCl	none	30 mM AS	no
stat	glycerol	none	5 mM H_2O_2	1 mM AS	yes
stat	glycerol	none	5 mM H_2O_2	30 mM AS	no
stat	glucose	none	none	1 mM AS	yes
stat	glucose	none	none	30 mM AS	no
stat	succinate	none	none	1 mM AS	yes

[1]AS: Ammonium sulphate, Gln: glutamine.

REFERENCES.

(1) Reitzer, L. Nitrogen assimilation and global regulation in *Escherichia coli*. *Annu Rev Microbiol*. **2003**, *57*, 155-176.

(2) Truan, D.; Huergo, L. F.; Chubatsu, L. S.; Merrick, M.; Li, X. D.; Winkler, F. K. A new P(II) protein structure identifies the 2-oxoglutarate binding site. *J Mol Biol*. **2010**, *400*, 531-539.

(3) Doucette, C. D.; Schwab, D. J.; Wingreen, N. S.; Rabinowitz, J. D. alpha-Ketoglutarate coordinates carbon and nitrogen utilization via enzyme I inhibition. *Nat Chem Biol*. **2011**, *7*, 894-901.

(4) Lienhardt, C.; Espinal, M.; Pai, M.; Maher, D.; Raviglione, M. C. What research is needed to stop TB? Introducing the TB Research Movement. *PLoS Med*. **2011**, *8*, e1001135.

(5) Amon, J.; Titgemeyer, F.; Burkovski, A. A genomic view on nitrogen metabolism and nitrogen control in mycobacteria. *J Mol Microbiol Biotechnol*. **2009**, *17*, 20-29.

(6) Mashego, M. R.; Rumbold, K.; De Mey, M.; Vandamme, E.; Soetaert, W.; Heijnen, J. J. Microbial metabolomics: past, present and future methodologies. *Biotechnol Lett*. **2007**, *29*, 1-16.

(7) Oldiges, M.; Lutz, S.; Pflug, S.; Schroer, K.; Stein, N.; Wiendahl, C. Metabolomics: current state and evolving methodologies and tools. *Appl Microbiol Biotechnol*. **2007**, *76*, 495-511.

(8) Behrends, V.; Bundy, J. G.; Williams, H. D. Differences in strategies to combat osmotic stress in *Burkholderia cenocepacia* elucidated by NMR-based metabolic profiling. *Lett Appl Microbiol*. **2011**, *52*, 619-625.

(9) Jozefczuk, S.; Klie, S.; Catchpole, G.; Szymanski, J.; Cuadros-Inostroza, A.; Steinhauser, D.; Selbig, J.; Willmitzer, L. Metabolomic and transcriptomic stress response of *Escherichia coli*. *Mol Syst Biol*. **2010**, *6*, 364.

(10) Tremaroli, V.; Workentine, M. L.; Weljie, A. M.; Vogel, H. J.; Ceri, H.; Viti, C.; Tatti, E.; Zhang, P.; Hynes, A. P.; Turner, R. J.; Zannoni, D. Metabolomic investigation of the bacterial response to a metal challenge. *Appl Environ Microbiol*. **2009**, *75*, 719-728.

(11) Snapper, S. B.; Melton, R. E.; Mustafa, S.; Kieser, T.; Jacobs, W. R. J. Isolation and characterization of efficient plasmid transformation mutants of *Mycobacterium smegmatis*. *Mol Microbiol*. **1990**, *4*, 1911-1919.

(12) Parish, T.; Wheeler, P. R. *Mycobacteria Protocols*; Humana Press: Totowa, 1998.

(13) Saikolappan, S.; Das, K.; Sasindran, S. J.; Jagannath, C.; Dhandayuthapani, S. OsmC proteins of *Mycobacterium tuberculosis* and *Mycobacterium smegmatis* protect against organic hydroperoxide stress. *Tuberculosis* **2011**, *91 Suppl 1*, S119-27.

(14) Bolten, C. J.; Kiefer, P.; Letisse, F.; Portais, J. C.; Wittmann, C. Sampling for metabolome analysis of microorganisms. *Anal Chem*. **2007**, *79*, 3843-3849.

(15) Kind, T.; Wohlgemuth, G.; Lee do, Y.; Lu, Y.; Palazoglu, M.; Shahbaz, S.; Fiehn, O. FiehnLib: mass spectral and retention index libraries for metabolomics based on quadrupole and time-of-flight gas chromatography/mass spectrometry. *Anal Chem*. **2009**, *81*, 10038-10048.

(16) Beckonert, O.; Keun, H. C.; Ebbels, T. M.; Bundy, J.; Holmes, E.; Lindon, J. C.; Nicholson, J. K. Metabolic profiling, metabolomic and metabonomic procedures for NMR spectroscopy of urine, plasma, serum and tissue extracts. *Nat Protoc*. **2007**, *2*, 2692-2703.

(17) Ulrich, E. L.; Akutsu, H.; Doreleijers, J. F.; Harano, Y.; Ioannidis, Y. E.; Lin, J.; Livny, M.; Mading, S.; Maziuk, D.; Miller, Z.; Nakatani, E.; Schulte, C. F.; Tolmie, D. E.; Kent Wenger, R.; Yao, H.; Markley, J. L. BioMagResBank. *Nucleic Acids Res*. **2008**, *36*, D402-8.

(18) Wishart, D. S.; Knox, C.; Guo, A. C.; Eisner, R.; Young, N.; Gautam, B.; Hau, D. D.;

Psychogios, N.; Dong, E.; Bouatra, S.; Mandal, R.; Sinelnikov, I.; Xia, J.; Jia, L.; Cruz, J. A.; Lim, E.; Sobsey, C. A.; Shrivastava, S.; Huang, P.; Liu, P.; Fang, L.; Peng, J.; Fradette, R.; Cheng, D.; Tzur, D.; Clements, M.; Lewis, A.; De Souza, A.; Zuniga, A.; Dawe, M.; Xiong, Y.; Clive, D.; Greiner, R.; Nazyrova, A.; Shaykhutdinov, R.; Li, L.; Vogel, H. J.; Forsythe, I. HMDB: a knowledgebase for the human metabolome. *Nucleic Acids Res*. **2009**, *37*, D603-10.

(19) Stein, S. E. An integrated method for spectrum extraction and compound identification from gas chromatography/mass spectrometry data *J Am Soc Mass Spectr*. **1999**, *10*, 770-781.

(20) Behrends, V.; Tredwell, G. D.; Bundy, J. G. A software complement to AMDIS for processing GC-MS metabolomic data. *Anal Biochem*. **2011**, *415*, 206-208.

(21) Jenkins, V. A.; Robertson, B. D.; Williams, K. J. Aspartate D48 is essential for the GlnR-mediated transcriptional response to nitrogen limitation in *Mycobacterium smegmatis*. *FEMS Microbiol Lett*. **2012**, *330*, 38-45.

(22) Behrends, V.; Ebbels, T. M. D.; Williams, H. D.; Bundy, J. G. Time-resolved metabolic footprinting for non-linear modelling of bacterial substrate utilization. *Appl Environ Microbiol*. **2009**, *75*, 2453-2463.

(23) Hunter, B. K.; Mowbray, S. L.; Walton, D. J. A compound representing the D-glycerate terminus of the methylglucose-containing polysaccharide of *Mycobacterium smegmatis*. *Biochemistry*. **1979**, *18*, 4458-4465.

(24) Kamisango, K.; Dell, A.; Ballou, C. E. Biosynthesis of the mycobacterial O-methylglucose lipopolysaccharide. Characterization of putative intermediates in the initiation, elongation, and termination reactions. *J Biol Chem*. **1987**, *262*, 4580-4586.

(25) Takenaka, F.; Uchiyama, H.; Imamura, T. Identification of alpha-D-glucosylglycerol in sake.

Biosci Biotechnol Biochem. **2000**, *64*, 378-385.

(26) Kaur, D.; Pham, H.; Larrouy-Maumus, G.; Riviere, M.; Vissa, V.; Guerin, M. E.; Puzo, G.; Brennan, P. J.; Jackson, M. Initiation of methylglucose lipopolysaccharide biosynthesis in mycobacteria. *PLoS One*. **2009**, *4*, e5447.

(27) Kramer, R. Bacterial stimulus perception and signal transduction: response to osmotic stress. *Chem Rec*. **2010**, *10*, 217-229.

(28) Klahn, S.; Steglich, C.; Hess, W. R.; Hagemann, M. Glucosylglycerate: a secondary compatible solute common to marine cyanobacteria from nitrogen-poor environments. *Environ Microbiol*. **2010**, *12*, 83-94.

(29) Elbein, A. D.; Pan, Y. T.; Pastuszak, I.; Carroll, D. New insights on trehalose: a multifunctional molecule. *Glycobiology*. **2003**, *13*, 17R-27R.

(30) Empadinhas, N.; da Costa, M. S. Diversity, biological roles and biosynthetic pathways for sugar-glycerate containing compatible solutes in bacteria and archaea. *Environ Microbiol*. **2011**, *13*, 2056-2077.

(31) Cox, R. A.; Cook, G. M. Growth regulation in the mycobacterial cell. *Curr Mol Med*. **2007**, *7*, 231-245.

(32) Smeulders, M. J.; Keer, J.; Speight, R. A.; Williams, H. D. Adaptation of *Mycobacterium smegmatis* to stationary phase. *J Bacteriol*. **1999**, *181*, 270-283.

(33) Wietzerbin-Falszpan, J.; Das, B. C.; Gros, C.; Petit, J. F.; Lederer, E. The amino acids of the cell wall of *Mycobacterium tuberculosis* var. *bovis*, strain BCG. Presence of a poly(L-glutamic acid). *Eur J Biochem*. **1973**, *32*, 525-532.

(34) Raunio, R. Accumulation of keto acids during the growth cycle of *Escherichia coli*. *Acta Chem*

Scand. **1966**, *20*, 11-16.

(35) Van Elsas, J. D.; Van Overbeek, L. S. *Starvation in Bacteria.*; Plenum Press: New York, 1993.

(36) Pope, C. F.; McHugh, T. D.; Gillespie, S. H. Methods to determine fitness in bacteria. *Methods in Molecular Biology*. **2010**, *642*, 113-121.

(37) Forsberg, L. S.; Dell, A.; Walton, D. J.; Ballou, C. E. Revised structure for the 6-O-methylglucose polysaccharide of *Mycobacterium smegmatis*. *J Biol Chem*. **1982**, *257*, 3555-3563.

(38) Griffin, J. E.; Gawronski, J. D.; Dejesus, M. A.; Ioerger, T. R.; Akerley, B. J.; Sassetti, C. M. High-resolution phenotypic profiling defines genes essential for mycobacterial growth and cholesterol catabolism. *PLoS Pathog*. **2011**, *7*, e1002251.

(39) Sassetti, C. M.; Boyd, D. H.; Rubin, E. J. Genes required for mycobacterial growth defined by high density mutagenesis. *Mol Microbiol*. **2003**, *48*, 77-84.
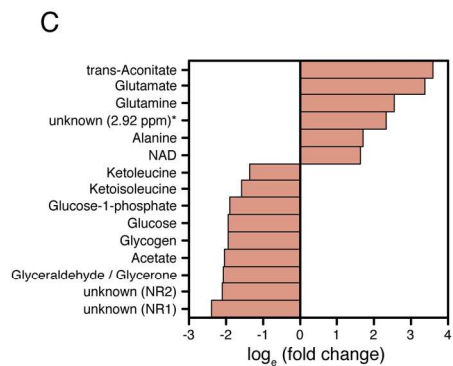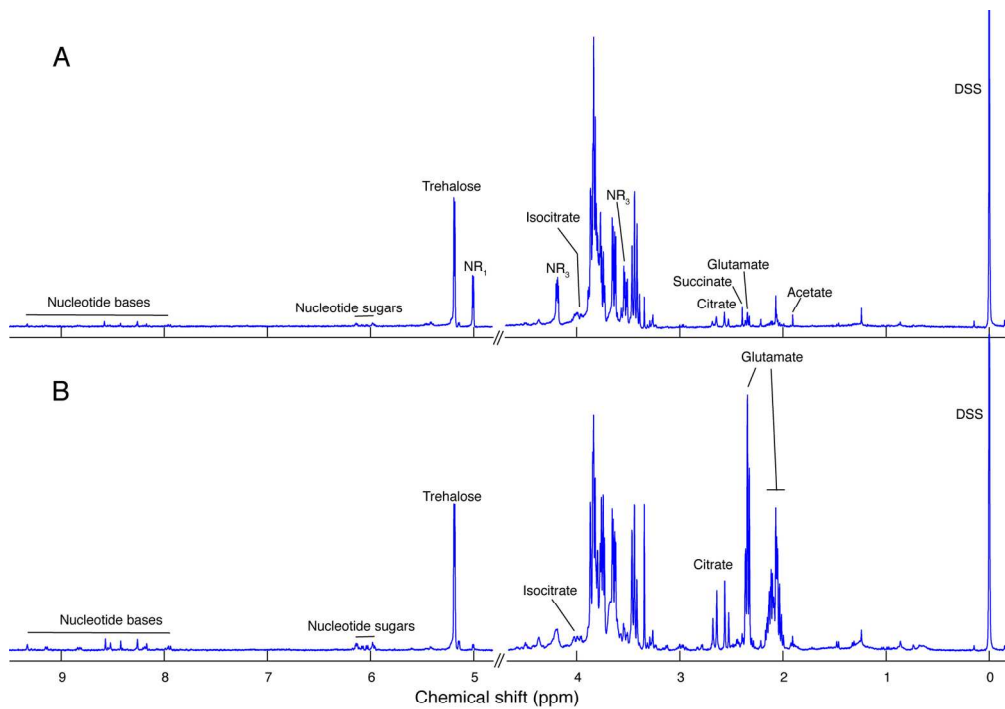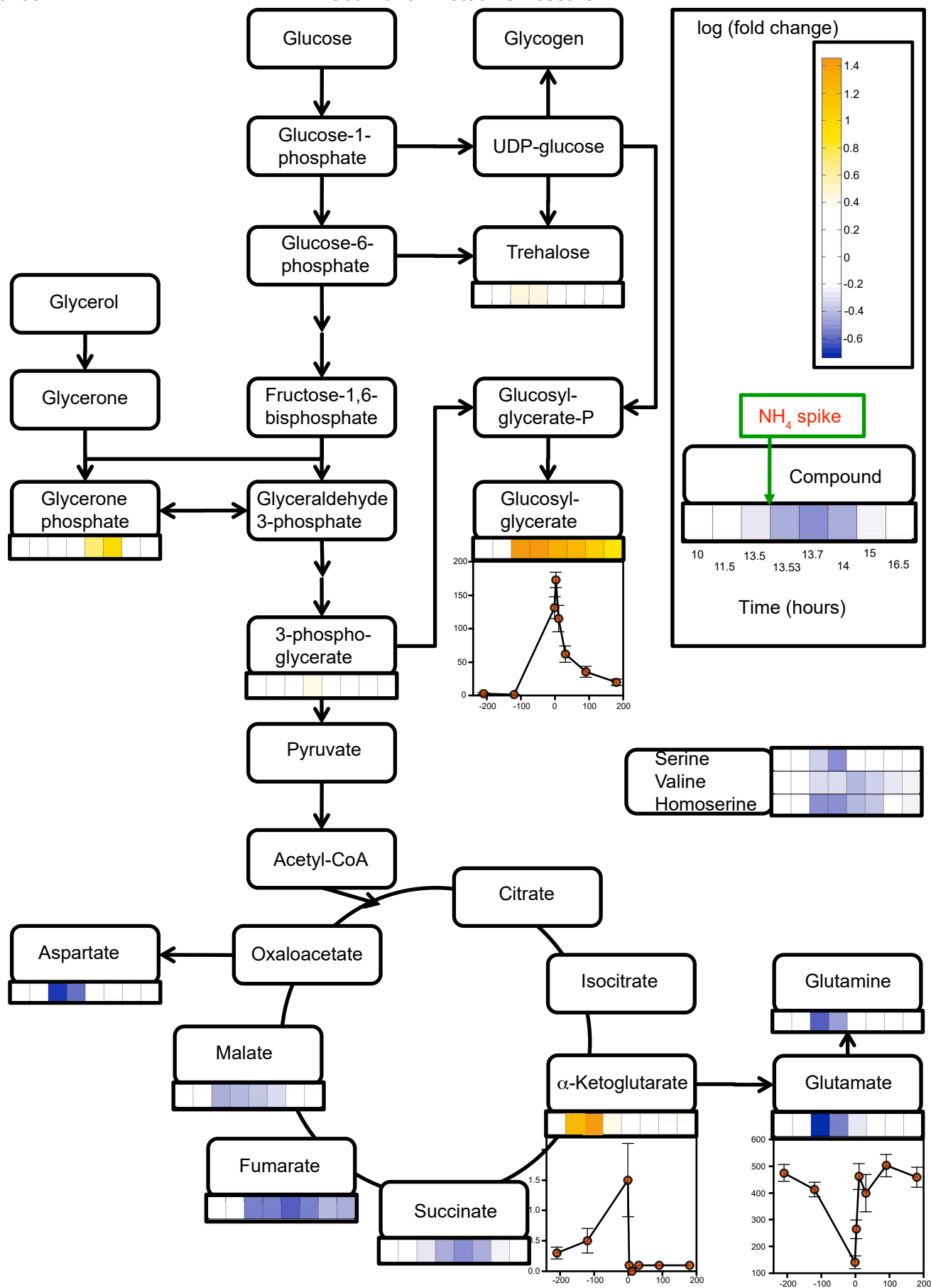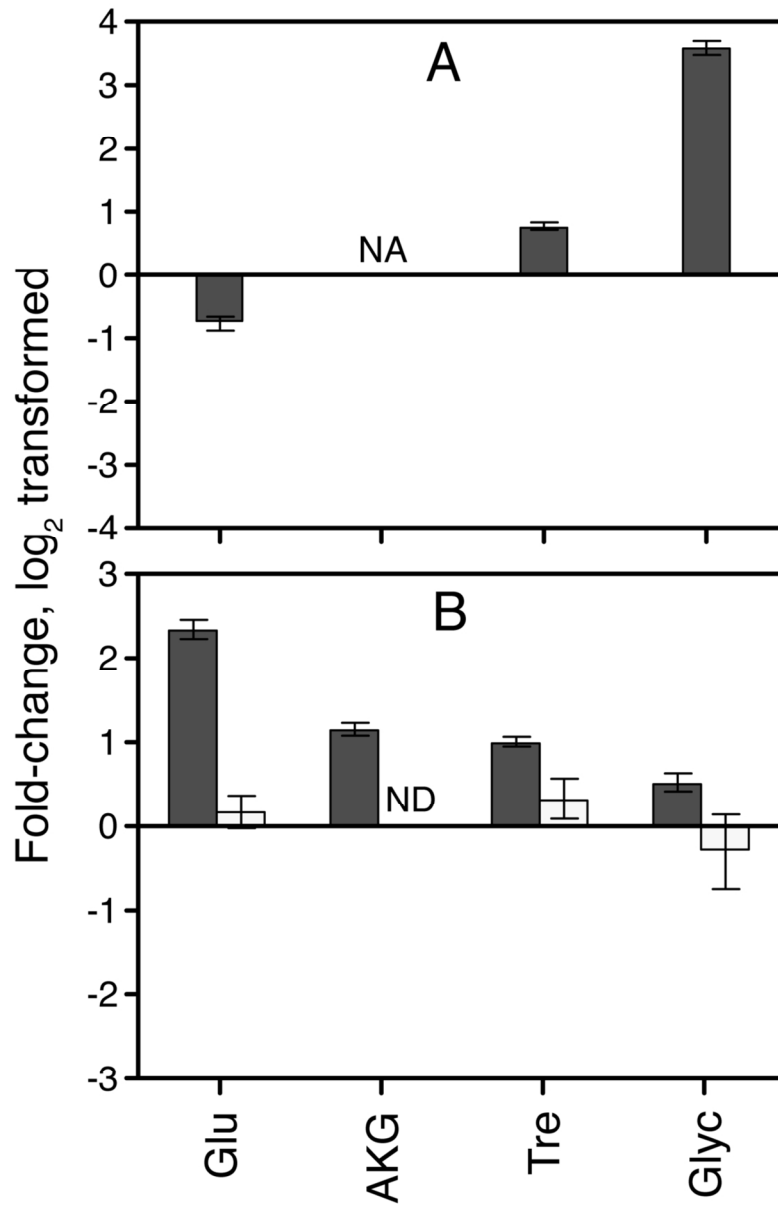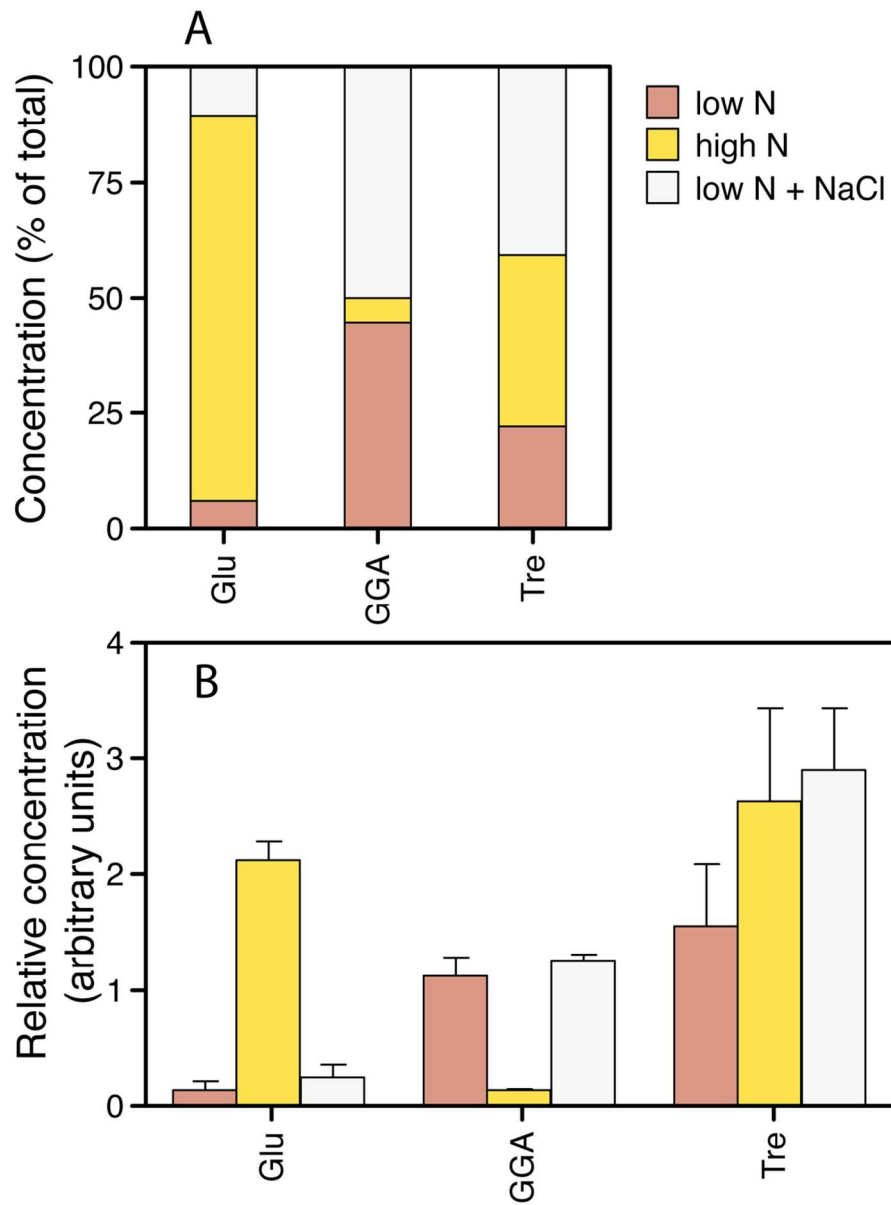
171x185mm (300 x 300 DPI)
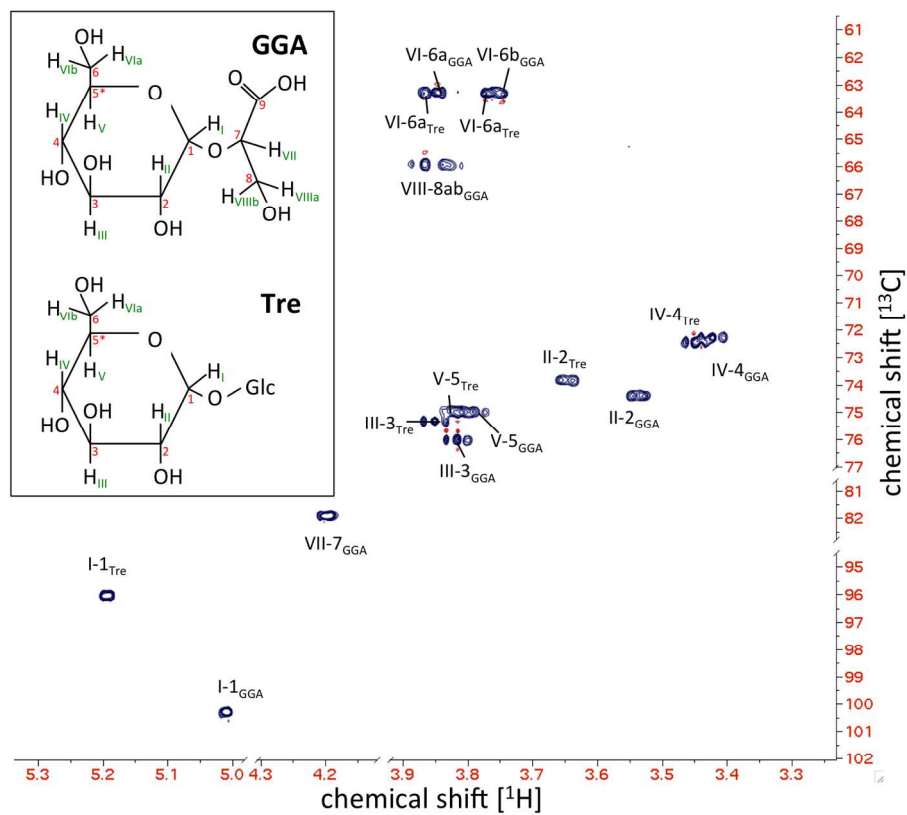
595x793mm (72 x 72 DPI)

94x145mm (300 x 300 DPI)

104x140mm (300 x 300 DPI)

TOC graphic
88x39mm (300 x 300 DPI)